Influences of Temperature Change Rates and Impervious Surfaces on the Intra-City Climatic Patterns of Busan Metropolitan Area*

Sun-Yurp PARK[1]※

부산광역시 국지적 기후 패턴에 대한 기온변화율과 불투수면의 영향*

박선엽[1]※

ABSTRACT

Influences of seasonal warming and cooling rates on the annual temperature patterns were analyzed based on the meteorological data from 13 weather stations in Busan Metropolitan Area(BMA), Korea during 1997~2014. BMA daily temperature time-series was generalized by Fourier analysis, which mathematically summarizes complex, regularly sampled periodic records, such as air temperature, into a limited number of major wave components. Local monthly warming and cooling rates of BMA were strongly governed by the ocean effect within the city. March(1.121℃ /month) and November(−1.564℃/month) were the two months, when the most rapid warming and cooling rates were observed, respectively during the study period. Geographically, spring warming rates of inland increased more rapidly compared to coastal areas due to weaker ocean effect. As a result, the annual maximum temperature was reached earlier in a location, where the annual temperature range was larger, and therefore its July mean temperature and continentality were higher. Interannual analyses based on average temperature data of all weather stations also showed that the annual maximum temperature tended to occur earlier as the city's July mean temperature increased. Percent area of impervious surfaces, an indicator of urbanization, was another contributor to temperature change rates of the city. Annual mean temperature was positively correlated with percent area of impervious surfaces, and the variations of monthly warming and cooling rates also increased with percent area of impervious surfaces.

요   약

　본 연구는 부산광역시 13개 기상관측지점을 대상으로 1997~2014년 동안의 기온상승율과 하강율의 계절적 특성이 연간 기온변화 특징에 미치는 영향을 분석하였다. 일별 기온 자료를 시계열적으로 단순화하기 위해 푸리에분석법을 적용하였는데, 이는 기상 자료와 같이 연속적으로 수집되는 시계열자료를 몇 개의 한정된 주요 파형으로 환원하여 자료를 단순화하는 수학적 기법이다. 부산광역시의 국지적 기온변화율은 대륙도에 의해 공간적으로 큰 영향을 받는 것으로 조사되었다. 계절적으로는 3월에 가장 높은 기온상승율(평균 1.121℃/month)을 보였고, 11월에 가장 가파른 기온하강율(평균 -1.564℃/month)을 나타냈다. 지역적으로 최난월인 8월 평균기온에 지배적인 영향을 주는 7월 평균기온상승율과 대륙도가 높은 지역일수록 최난일이 일찍 출현한 것으로 보아, 해양의 영향이 적은 지역일수록 기온상승률이 높고 해양 인접 지역에 비해 연중최고기온에 도달하는 시기가 앞당겨지는 것으로 분석되었다. 연구 지역 관측 지점 전체를 평균한 연도별 분석 결과도 7월 평균기온이 높은 해일수록 최난일 출현은 시기적으로 앞당겨지는 경향을 나타냈다. 도시화 정도를 나타내는 불투수면의 면적 비율 역시 기온의 연 변화와 통계적으로 상관관계를 갖는 것으로 나타났다. 관측지점의 불투수면 면적비율이 증가할수록 연평균기온이 높게 나타났고, 연평균 기온상승율과 하강율의 장기적 변동 폭도 크게 나타났다.

주요어 : 푸리에분석, 기온상승율, 기온하강율, 대륙도, 불투수면

INTRODUCTION

　Signals of climate change are substantially strong in Northeast Asia. Temperature increases in the region has been reported above the global average, and the temperature difference between winter and summer seasons has decreased significantly (NIMS, 2010; IPCC, 2013). Spatiotemporal changes of seasonal patterns and extreme phenomena such as annual maximum and minimum temperatures are important consequences of the climate change(Jung *et al.*, 2002; Choi, 2004; Choi *et al.*, 2006; Choi *et al.*, 2008; Cheng *et al.*, 2012). Research results indicated that peaks of annual temperature curves have moved forward in mid- and high-latitude regions (Thomson, 1995; Stine *et al.*, 2009).

Seasonal analyses of long-term data also showed a clear warming trend in Korea. For example, winter temperature increased much faster than summer temperature, and it reduced annual temperature ranges significantly. Annual mean temperature continued to increased over the past several decades, and the warming trend was observed in all major cities of the nation(Choi, 2004; Choi *et al.*, 2008; Jin and Park, 2015).

　Rapid urban sprawl of Busan Metropolitan Area(BMA) has been widespread and intensive since 1980s(Park and Baek, 2009; Jin and Park, 2015). Urbanization inevitably leads to substantial transformation of land uses, and it is tightly associated with deforestation and removal of agricultural land, resulting in the landscape structure changes of built-up area, agricultural area,

and forests. From ecological and climatic perspectives, large-scale urbanization not only changed the landscape structure of a city but also caused changes in surface energy balances of the urban ecosystem, degrading various environmental functions in terms of energy exchanges, water budget, and regulation of air temperature and humidity(Hong and Lee, 1997; Pielke et al., 2002; Feddema et al., 2005; Jung et al., 2005; Coutts et al., 2007; Deng et al., 2013).

Increases in annual or seasonal mean temperatures are an obvious indication of climatic warming in urban environments. However, the magnitude of warming or cooling varies geographically, and the slope of temperature changes also varies seasonally. Particularly, seasonal warming and cooling rates in a coastal region can be intimately influenced by the ocean effect on a local scale(Jin and Park, 2015). Therefore, the slope of temperature changes in a given season may change spatially, and it strongly relates to seasonal climatic characteristics including annual extreme temperatures and the day of maximum temperature(Choi, 2004; Choi et al., 2008; Qian et al., 2012). Since BMA's urbanization was uncomparably broader and faster than surrounding regions, the climatic influence of impervious surfaces as a characteristic feature of urbanization is locally expected in the city (Seto and Fragkias, 2005; Ahn et al., 2012; Park and Tak, 2013). Urban sprawl and its relationship with climatic warming has been recently reported in the study area(Park and Tak, 2013; Kim et al., 2014). However, local-level, intracity analyses of warming or cooling patterns

still remain unclear. Located in the southernmost coast, BMA is subject to an environmental transition to subtropical climate, and the city's preparedness for summer heat waves, energy management, temperature-related health and environmental hazards is urgent(Kwon et al., 2007; Kim et al., 2014; Lee et al., 2014; Lee and Lee, 2016). Considering the heterogeneous characteristics of the city's landscape structure, detailed investigation of the uneven patterns of annual temperature changes within the city is needed. This study was conducted to determine the influence of monthly warming and cooling rates on the annual temperature patterns, including the days of maximum and minimum temperatures in relation to impervious surface in BMA using daily air temperature records during 1997~2014.

MATERIALS AND METHODOLOGY

1. Study Area

Busan Metropolitan Area(BMA) was selected as a study area. The city is located at the southeastern edge of the Korean peninsula and it is the second largest city in the nation with its population of 3.5million (FIGURE 1). The climate of the city is classified as humid subtropical winter-dry climate, and the city is hot and wet in summer and cold and dry in winter. The city's annual mean temperature and total precipitation are 14.7℃ and 1,519㎜, respectively. While 51% of annual total precipitation is concentrated from June to August, winter precipitation is only 7% of the total precipitation. As the largest port city of the nation, BMA is the economic,
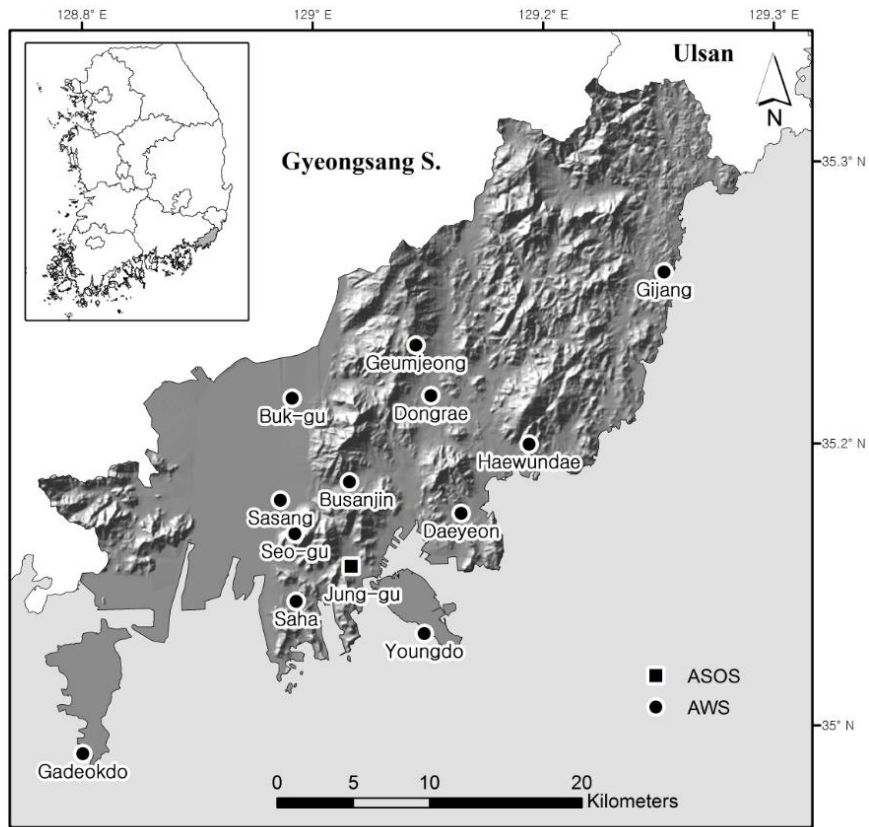
FIGURE 1. Study area. A shaded-relief map is draped over the area

educational, and cultural center in the southeastern region of the country. The city's population is primarily distributed in the central part of the city along a narrow valley surrounded by numerous mountains with the highest peak of 801meters above the sea level. The western part of BMA is agricultural plains and industrialized districts, and the eastern area is largely covered by forests. About 43% of BMA's total area is covered by forests, and agricultural fields are the second largest(14.3%) land use type of the city.

2. Datasets

Daily air temperature data from 1997 to 2014 were acquired from 12 automatic weather systems(AWS) and 1 automatic synoptic observing system(ASOS) managed by the Korea Meteorological Administration (KMA). Gapless, 18-year long data were available for ten locations, but temperature data were available for a limited number of years ranging from 13 years to 17 years for three locations(TABLE 1). From each weather station, minimum, maximum, and mean temperatures were collected and analyzed. Land use and land cover data were extracted from the city's biotope map produced by Busan Development

TABLE 1. Data collection periods and site information for each weather station

Location	Period	Latitude (° N)	Longitude (° E)	System	Elevation (m)
Jung-gu	1997~2014	35.10	129.02	ASOS	70
Seo-gu	1997~2014	35.12	128.98	AWS	517
Sasang	1997~2009	35.14	128.97	AWS	4
Youngdo	1997~2014	35.05	129.07	AWS	137
Gadeokdo	1998~2014	34.98	128.82	AWS	73
Gijang	1997~2014	35.27	129.25	AWS	65
Haewundae	1997~2014	35.17	129.15	AWS	62
Busanjin	1997~2014	35.15	129.02	AWS	108
Geumjeong	1997~2014	35.23	129.07	AWS	75
Dongrae	1997~2014	35.20	129.08	AWS	71
Buk-gu	1997~2014	35.20	128.98	AWS	34
Daeyeon	1997~2014	35.13	129.10	AWS	14
Saha	2002~2014	35.08	128.98	AWS	138

Institute(BDI). Biotope is a synonymous term with habitat, and it is defined as an area of environmental conditions suitable for a specific assemblage of plants and animals. Based on the map's classification scheme, impervious surfaces were precisely defined as terrestrial, man-made, and non-vegetated impervious surfaces(BDI, 2010). Impervious surfaces are areas covered by materials that impede the infiltration of water into the soil. Buildings, pavement, concrete, and parking lots are typical examples of impervious surfaces. Amounts of impervious surfaces in urban areas have significant impacts on water quality, biological activities, flood management, and urban climate(Stone and Rodgers, 2001; Brabec et al., 2002; Jennings and Jarnagin, 2002; Coutts et al., 2007).

3. Time-Series Analysis: Fourier Analysis

Fourier analysis, or harmonic analysis, is a useful method for researchers to determine representative periodicity embedded in time-series data that follow a repetitive, cyclic pattern, such as air temperature. Fourier analysis effectively simplifies the input data by extracting a limited number of major wave forms from regularly-sampled data or signals(Andres et al., 1994; Olsson and Eklundh, 1994; Azzali and Menenti, 2000; Jakubauskas et al., 2001; Davis, 2002; Park, 2003; Park, 2009; Park, 2011; Wilks, 2011). More technically, the method mathematically decomposes a complex time series into its constituent parts and transforms the time series to a sum of numerous wave functions, or harmonic terms. Each of these harmonic terms represents a periodic, repeating pattern of a phenomenon with a unique set of amplitude, wavelength, and phase angle. Since the original raw curve is the sum of all successive harmonic terms and the mean, the more harmonic terms are added, the closer the resulting curve becomes to the original time-series. A basic equation of these trigonometric relationships is summarized below(Olsson and Eklundh, 1994; Jakubauskas et al., 2001):
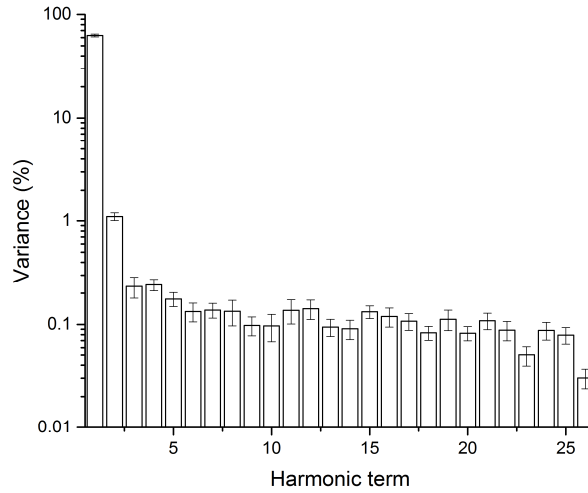
FIGURE 2. Percent variances of the successive harmonics

$$f(x) = f(x)_{mean} + \sum_{k=1}^{k=N/2} (a_k \sin(\frac{2\pi k}{P})$$
$$+ b_k \cos(\frac{2\pi kx}{P}))$$

It is assumed that one complete wave form of a simple cosine curve has an interval of 2π for the year. f(x)mean is the mean of the whole time-series. The subscript k is called the harmonic number or the frequency of the curve per interval. N is the number of observations in the time-series, and P is the fundamental period of the data (e.g. P=52 if data are treated weekly). Two Fourier coefficients, a_k and b_k, are defined as:

$$a_k = \frac{2}{N} \sum_{x=1}^{x=N} (f(x)\sin(\frac{2\pi kx}{P}))$$
$$b_k = \frac{2}{N} \sum_{x=1}^{x=N} (f(x)\cos(\frac{2\pi kx}{P}))$$

The harmonic equation states that any complex time-series can be expressed as the sum of a series of cosine curves. The total variance of the input time series equals to the sum of the variances of all harmonics produced by Fourier analysis. Therefore, the percent variance of an individual harmonic term indicates the proportion of the total variance of the time series. The percent variance of each harmonic term decreased dramatically as the rank of a harmonic term declined (FIGURE 2). Typically, the most important harmonic terms of a time-series are the first few ones that explain most of variance of the input data. For instance, the first harmonic term of temperature data represents a wave form that completes one single cycle during a year, and it is the dominant periodic component of annual temperature changes (Park, 2010). The first four harmonic terms, which were used in the analysis, explained more than 95% of the input data with the range of 95.7%~97.2%. FIGURE 3 shows an example of the four major harmonic terms combined for Haewundae using its time-series data for four selected years.
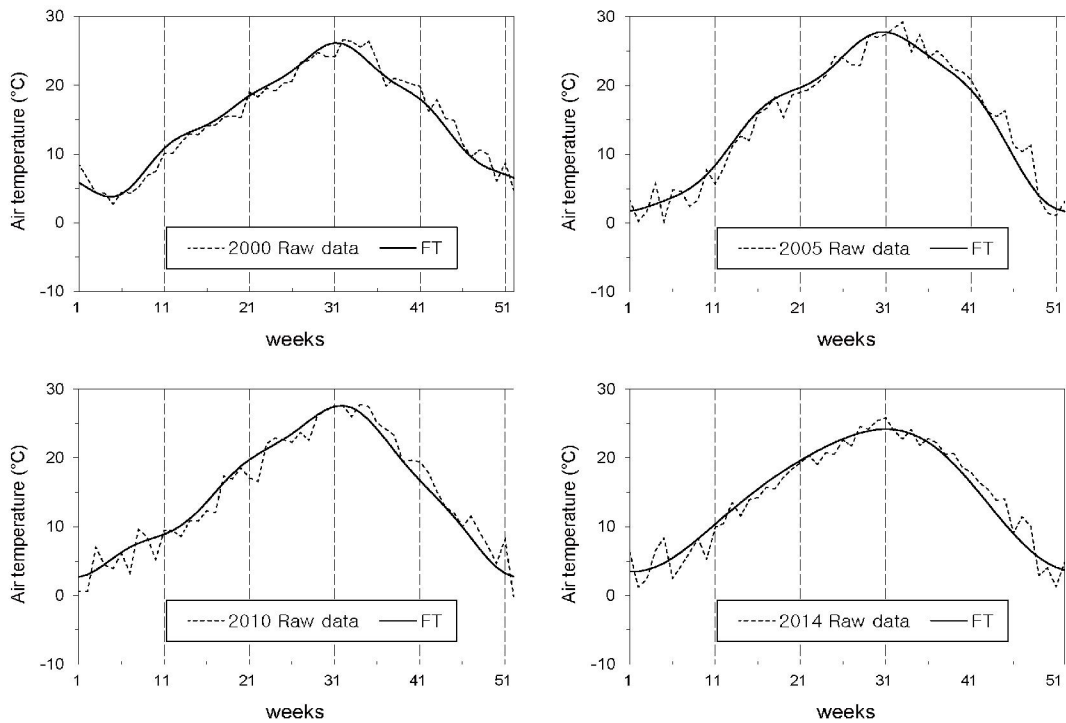
FIGURE 3. Results of Fourier analysis at Haewundae
(data in 2000, 2005, 2010, and 2014 were shown as an example).
Raw temperature data were smoothed out and simplified by Fourier transformation (FT)

4. Slope of Temperature Change
: The First Derivative

Differentiation is a mathematical process that computes a derivative of a function of a real variable. By definition, a first derivative of a function at a chosen independent value, x, is a slope of the tangent line to the function at the point x. Since the tangent line to the function is the best linear approximation at the given point in terms of its slope, the first derivative often represents the instantaneous rate of change, describing how much the function is increasing or decreasing at the given point. For example, the derivative of a function y=f(x) of a independent variable

x is a measure of the rate at which the dependent value y of the function changes with the change of the independent variable x. Therefore, differentiation, a process of finding a derivative, can be used to determine how rapidly an independent variable increases or decreases at a specific point of a function. A positive derivative indicates that the function f(x) increases with the increases of the independent variable x. A negative derivative indicates that the function f(x) decreases with the increases of the independent variable x. In notation, the derivative of y with respect to x is expressed as $\frac{dy}{dx}$ or f'(x) indicating

the ratio between the two infinitesimal quantities. The raw air temperature time-series was simplified by Fourier analysis, and then the temperature curve was used as a function and differentiated to compute the first derivative for each day. Daily temperature increasing or decreasing rates were finally averaged and integrated into monthly values. When the derivative reaches 0 at a given day, it becomes the local maximum or a local minimum at that point during the year because the slope is not positive or negative.

RESULTS AND DISCUSSION

1. Seasonal Warming and Cooling Rates

Seasonal analysis results showed that the highest warming rate was observed in spring followed by summer and winter while a continuous cooling mode was found in the fall season ranging from September to November(FIGURE 4a and TABLE 2). The highest warming rate was observed in March(1.121℃/month) regardless of observation points. After the annual maximum temperature, the cooling rate continued to decrease and reached the most rapid cooling in November(−1.564℃ /month). A seasonal climatic pattern was typically represented and characterized by a rapid spring warming and a fall cooling across the city. However, inter-annual trends or patterns were not found during the study period.

The city's warmest and coldest months are August and January, and monthly mean temperatures of these two months were significantly influenced by the warming and cooling rates of July and September, respectively(FIGURE 4b). Comparative analyses of monthly warming and cooling rate curves clearly showed that temporal patterns of seasonal warming and cooling rates varied spatially. In other words, temporal progressions of local warming and cooling differed from place to place. The city's annual maximum temperatures were observed between July 26 and August 19 during 1997~2014. The mean temperature of August, the warmest

TABLE 2. Mean temperature (Tmean), maximum warming rate (warming_max), maximum cooling rate (cooling_max), and continentality of each location (1997~2014)

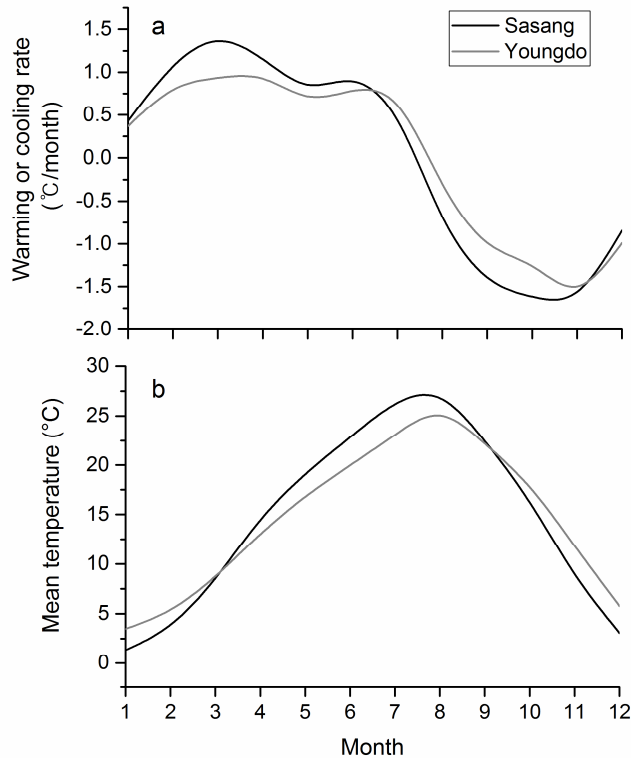| Location	Tmean(℃)	warming_max(℃/month)	cooling_max (℃/month)	continentality
Jung-gu	14.9	1.039	−1.554	40.2
Seo-gu	11.6	1.199	−1.646	43.8
Sasang	14.5	1.364	−1.560	47.1
Youngdo	14.4	0.934	−1.499	37.8
Gadeokdo	14.7	1.022	−1.520	39.2
Gijang	14.3	1.128	−1.509	41.0
Haewundae	15.1	1.016	−1.516	39.1
Busanjin	15.0	1.156	−1.628	43.9
Geumjeong	14.6	1.191	−1.555	44.1
Dongrae	15.1	1.162	−1.572	42.7
Buk-gu	14.4	1.221	−1.588	43.9
Daeyeon	15.3	1.101	−1.601	42.5
Saha	15.0	1.043	−1.586	41.3

FIGURE 4. Monthly temperature change rates
(a) and mean temperature (b). Two locations with the
highest (Sasang) and lowest (Youngdo) continentality
are provided as an example

month, increased as the warming rate of July increased(FIGURE 5). From the temporal perspective, interannual analyses based on average temperature data of all weather stations also revealed that the higher the city's average temperature in July, the earlier the phase value, the equivalent to the day of maximum temperature, appeared during the year (r=−0.662). Annual minimum temperature was observed as early as October 20 and May 10 at the latest during the study period. The impact of monthly cooling on the coldest month(January) was found greatest in September. The more rapid

(more negative) the cooling rate of September, the lower the mean January temperature with the correlation coefficient of r=0.543. Unlike the warming rate in summer, the cooling rate of September did not have a meaningful correlation with the day of minimum temperature. In addition, the annual maximum and minimum temperatures only had a weak correlation with June(r=0.379) and September(r=0.316) mean temperatures, respectively.

2. Ocean Effect on Temperature Changes
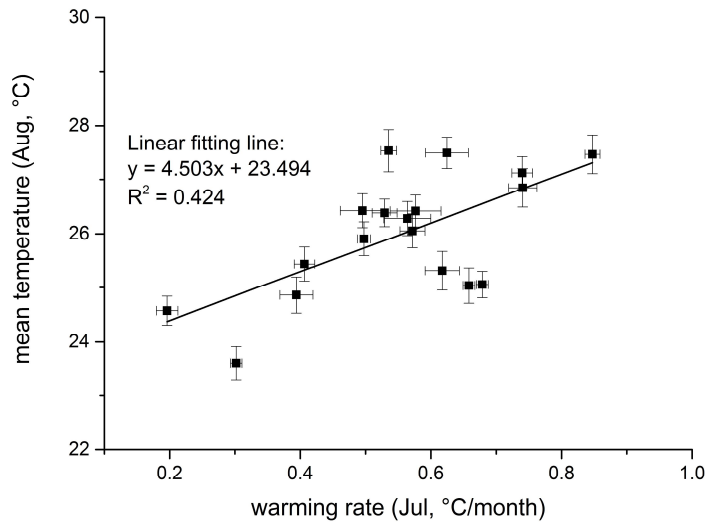
Local variations of warming and cooling

FIGURE 5. Correlation between July warming rate and
August mean temperature

rates in BMA were intimately associated with annual temperature ranges. The speed of warming varied geographically, and it was strongly influenced by the ocean effect. Temperature typically increased more rapidly, and a warming-to-cooling phase transition took place earlier in the interior compared to coastal locations. Therefore, the annual maximum temperature appeared earlier in a place, where the ocean effect was weaker including Sasang, Bukgu, and Geumjeong. Once the annual peak temperature was reached, temperature of the interior locations started to decrease earlier than that of coastal areas. As a result, warming rates of the interior and coastal areas were reversed in July, and interior locations cooled more rapidly than coastal locations beginning in August. Phase and amplitude values of the first harmonic terms computed by Fourier analysis accurately demonstrated the relationship between annual temperature fluctuations (amplitude) and the day of

annual maximum temperature(phase). In fact, annual temperature ranges and the day of annual peak temperature were well represented by mean amplitude and phase values during the study period. As shown in FIGURE 6, phase values typically belonged to mid- to late-July, and they were negatively correlated with mean July temperature. As a result, the julian day of the annual maximum temperature decreased as July mean temperature increased.

The influence of the ocean can be quantified by continentality(K), and continentality of a location is a function of the latitude and annual temperature range of that location. Continentality was computed using the well-known Gorzynsky's method(Hidore et $al.$, 2010):

K = 1.7(A/sin ϕ) - 14
(A= annual temperature range, ϕ =latitude)
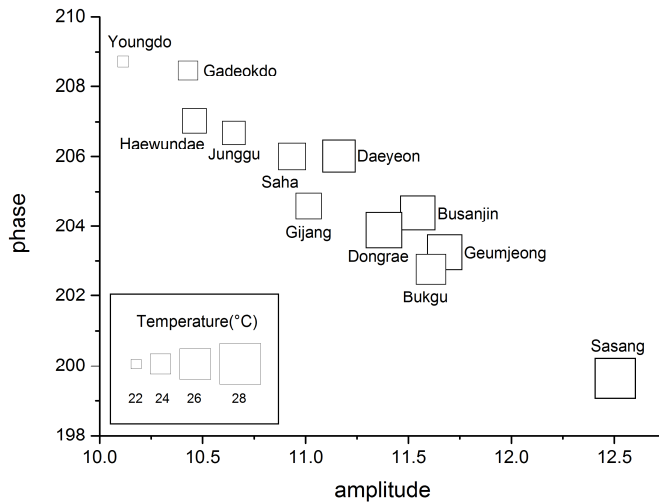
Although BMA is a typical coastal city

FIGURE 6. Mean values of phase(julian day) and amplitude(℃) of the first
harmonic term from Fourier analysis for each location.
July mean temperature is represented by the square size and
it is compared with phase and amplitude for each location

in the southeast, the city's continentality varied locally from 37.8 to 47.1. The warming phase began in January for all locations, and the highest warming rate was found in March. Geographically, inland areas with higher continentality had more rapid warming rates in spring than coastal areas. Due to the geographical difference in warming rates, occurrence of annual maximum temperatures varied spatially. In locations, where continentality is high, spring warming rates were higher and the maximum temperature appeared earlier than those with low continentality. In short, the annual temperature range increased as the spring warming rate became steeper and the annual maximum temperature was reached earlier during the year. Local cooling rates were also influenced by continentality. Since rapid warming and cooling were intimately associated with large annual temperature

ranges, monthly warming and cooling rates were strongly correlated with each other (FIGURE 7a). Although the cooling rates of fall were steeper in locations with high continentality, a statistically meaningful correlation was not found between the cooling rates and the day of annual minimum temperature(FIGURE 7b). On a regional scale, it was reported that seasonal air temperature variations were influenced by sea surface temperatures (SST) over the Korean peninsula(Kang and Suh, 1986). Since the relationship between air temperature and SST are dependent upon time and space, the impact of SST on the local-scale variations of air temperature across the study area remains uncertain and should be further assessed.

3. Impacts of Impervious Surfaces

Urban area, forest, and agricultural land are three primary land uses, and they
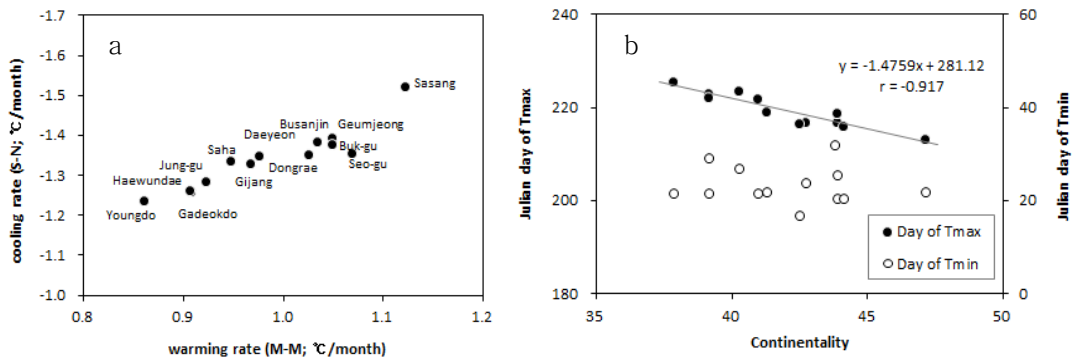
FIGURE 7. Correlation(r=−0.926, p<0.01) between spring warming rates and fall cooling rates in the Busan Metropolitan Area (a). Julian days of annual maximum(Tmax) and minimum(Tmin) temperatures recorded in each weather station were compared to their continentality (b)

amount to 89% of the total area of the city as of 2010(BDI, 2010). The landscape structure of BMA was significantly changed for the past three decades. Urban area of BMA has greatly increased by 280.9% since 1980. While urban area increased dramatically, agricultural and forest area has been diminished to 48.2% and 85.1% of that in 1980. During the 1980~2010 period, 14.3%(6,246ha) of the entire forest area of BMA was transformed to urban area or agricultural land. In addition, 50.3%(10,720.4ha) of the city's agricultural land was changed to urban area or forest. In summary, 45.5% (9,697.4ha) of forest and 58.2%(7,373ha) of agricultural land were transformed to urban area. From the viewpoint of landscape structure, the rapid urban sprawl has resulted in significant growth of urban area patches, which typically consists of impervious surfaces. Increases of large urban patches were due to merging and connection of existing patches caused by rapid urbanization(Park and Tak, 2013).

Percent area of impervious surface can be regarded as an indirect measure of urbanization, and impervious surfaces are estimated 25.4% of the entire city area as of 2010(BDI, 2010). The spatial structure of impervious surfaces varied across the study locations, and its percent area ranged from 0% to 85%(FIGURE 8). Highly urbanized areas, such as Busanjin, Jung-gu, and Dongrae, were covered mostly by impervious surfaces(75%~85%). By contrast, percent area of impervious surfaces of central mountainous areas (Geumjeong and Seo-gu) and eastern coastal areas(Gijang, Haewundae, and Youngdo) was significantly lower ranging from 7% to 31%. Percent impervious surface area had significant correlations with the city's mean air temperature and monthly variations of air temperature. Annual mean temperatures had a significant positive correlation with the percent area of impervious surfaces (r=0.600). This temperature-impervious surface relationship increased as the buffer distance from each location increased from
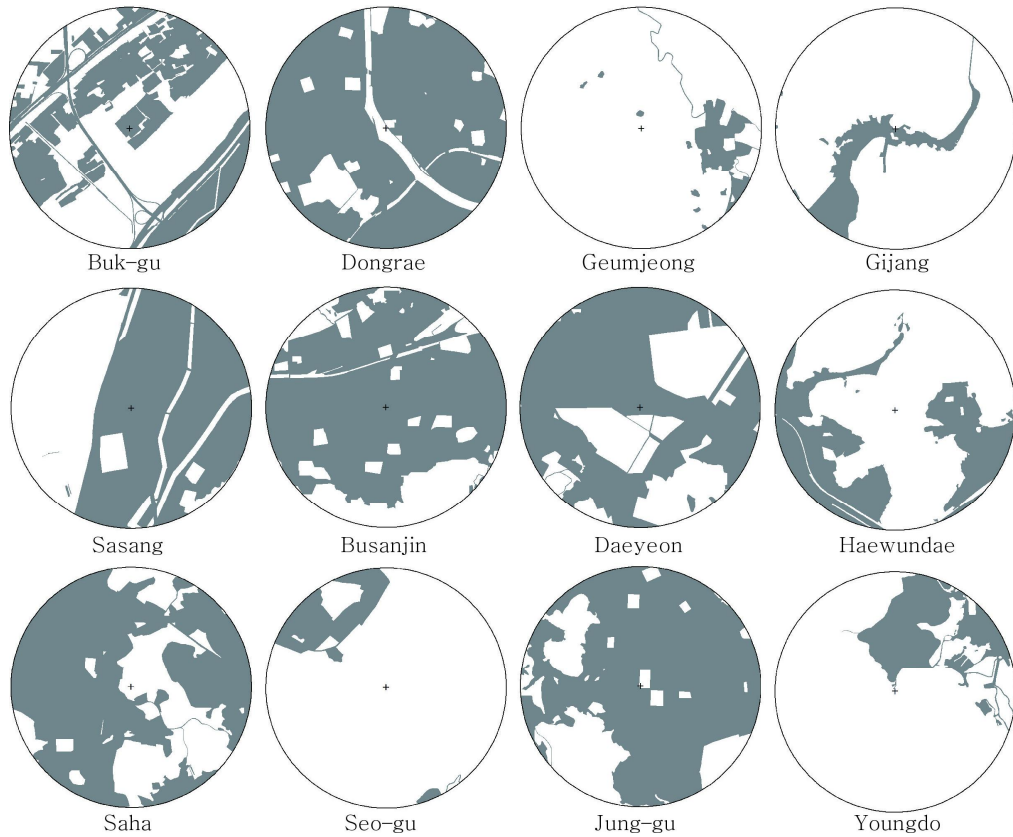
FIGURE 8. Impervious surfaces (shaded area) are mapped within a 1 km-radius circle around each weather station except Gadeokdo, where no impervious surface was mapped

100 meters to 1 kilometer with an increment of 100 meters. The effective radius from a weather station seems to influence the annual mean temperature of that location, but further investigation is needed to better understand the impact of the spatial domain on air temperature. Standard deviations(1997~2014) of warming (February ~June, r=0.533) and cooling (September~December, r=0.560) rates also had positive correlations with percent impervious surface area(FIGURE 9). This result showed that thermal properties of impervious surfaces as a characteristic variable contributed to intra-city variations of mean temperature and interannual fluctuations of warming and cooling rates.

On a regional scale, it was reported that long-term temperature increases were faster in inland regions compared to coastal regions(Park and Tak, 2013). The present study showed that annual mean temperatures and temperature change rates were strongly responsive to the degree of urbanization represented by impervious surface area across the city. Considering the importance of thermal characteristics of urban landscape, information on land cover changes should be carefully evaluated in the future climatic impact assessment
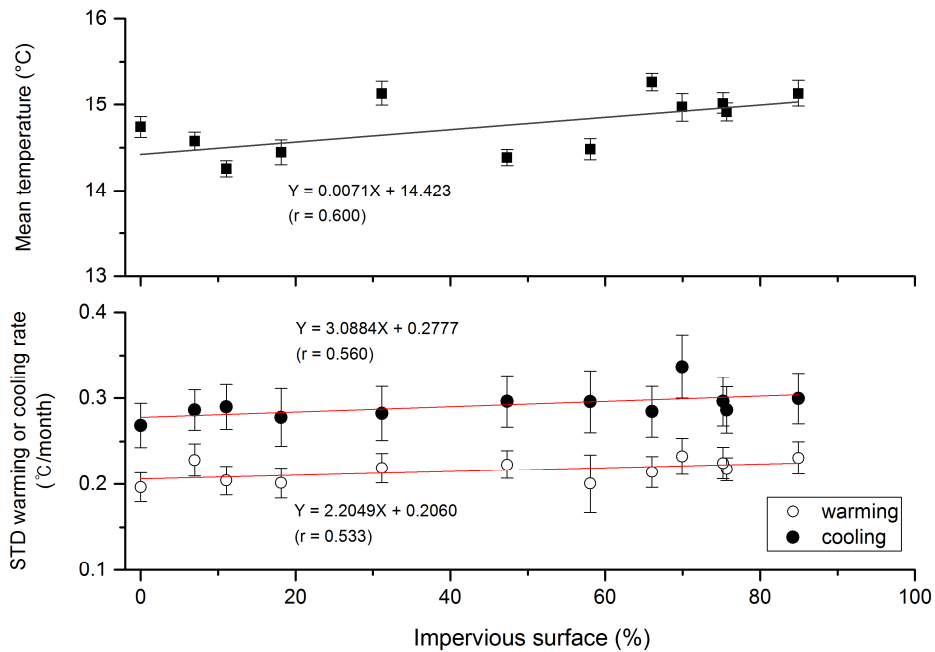
FIGURE 9. Percent area of impervious surface within 1 km radius of each location and its corelation with mean temperature(upper panel) and standard deviations(STD) of warming and cooling rates(lower panel) at 12 weather stations. Significantly low outlier temperature at Seo-gu(mountain-top location of 517 m above the sea level) was excluded

(Bierwagen *et al*., 2010). For example, the urbanization has contributed to 50% of the increase of land surface temperature in the USA since 1950(Stone Jr., 2009). Urbanization quickly triggers landscape transformation from vegetated area to impervious surfaces and reduces urban green area. Vegetation greenness has been known for its contribution to weaker spring warming due to the evaporative cooling effect on a regional scale in East Asia(Jeong *et al*., 2009). Therefore, urbanization may accelerate the spring warming rate and enhance the intensity of heat waves, reducing evapotranspiration from land surfaces (Owen *et al*., 1998; Kondoh and Nishiyama, 2000). BMA's persistent urban sprawl may contribute to the local expansion of impervious surface and the city's climate change in the long run.

CONCLUDING REMARKS

Generalization of regularly-sampled time -series by Fourier analysis was an effectively way to summarize complex, long -term temperature records. Based on the smoothed temperature curves, the instantaneous rate of temperature change was successfully computed. Although impacts of urbanization on climate have been commonly reported on a city, regional, or broader level, more detailed, intracity-scale climate studies are still rare. Urban development and natural environment of BMA has been substantially

dynamic for decades, but the intracity-level investigation of local climate change was limited partly due to the lack of meteorological and land use data. Analyses of recent 18-year long temperature data of BMA showed that the most rapid warming and cooling rates were observed in March and November, respectively at all locations during the study period. However, the slope of monthly warming and cooling differed from place to place within the city. Intracity-level temperature change rates of BMA varied geographically and were strongly governed by the ocean effect at a location considered in the city. The ocean effect is inversely correlated with the annual temperature range, which was quantitatively expressed by continentality. Spring warming rates increased more rapidly at a location, where continentality was higher, and the annual maximum temperature was reached earlier at that location. That is, a large annual temperature range was associated with high continentality and an early annual maximum temperature. July warming rate had a strong positive correlation with August mean temperature, the warmest month of the year, and July mean temperature was negatively correlated with the julian day of the annual maximum temperature. Geographically, local continentality had an almost linear relationship(r=−0.917) with the julian day of the annual maximum temperature. Impervious surface area, an indicator of urbanization, was another contributor to temperature change rates of the city. The positive relationship between percent area of impervious surfaces and annual mean temperature within the city indicated that urbanization-induced warming was linked with weakening of the evaporative cooling effect of vegetation as well as the urban heat island effect. In summary, this study provides two main implications for future climate change on a local scale. Firstly, monthly warming and cooling rates varied spatially even on the intracity scale, and the time of annual maximum temperatures were correlated with the spatial warming patterns. Secondly, variations of monthly warming and cooling rates were attributed to the urbanization-derived increase of impervious surfaces. Since urban sprawl reduces an evaporative cooling effect in a city, urbanization plays an important role in seasonal temperature change patterns in both temporal and spatial dimensions in BMA. In addition, direct linkage between ground observations and sea surface temperature around the city should be further investigated in the future because the ocean effect is clearly influential in local climate as a governing factor in the city. **KAGIS**

REFERENCES

Ahn, J.S., J.D. Hwang, M.H. Park, and Y.S. Suh. 2012. Estimation of urban heat island potential based on land cover type in Busan using Landsat-7 ETM+ and AWS Data. Journal of the Korean Association of Geographic Information Studies 15(4):65-77 (안지숙, 황재동, 박명희, 서영상. 2012. Landsat-7 ETM+ 영상과 AWS 자료를 이용한 부산의 토지피복에 따른 여름철 도시열섬포텐셜 산출. 한국지리정보학회지 15(4):65-77).

Andres, L., W.A. Salas, and D. Skole. 1994. Fourier analysis of multi-temporal

AVHRR data applied to a land cover classification. International Journal of Remote Sensing 15(5):1115−1121.

Azzali, S. and M. Menenti. 2000. Mapping vegetation−soil−climate complexes in southern Africa using temporal Fourier analysis using NOAA−AVHRR−NDVI data. International Journal of Remote Sensing 21(5):973−996.

BDI (Busan Development Institute). 2010. Urban biotope mapping of the central region, Busan. Busan Metropolitan City.

Bierwagen, B.G., D.M. Theobald, C.R. Pyke, A. Choate, P. Groth, J.V. Thomas, and P. Morefield. 2010. National housing and impervious surface scenarios for integrated climate impact assessments. Proceedings of the National Academy of Sciences 107(49):20887−20892.

Brabec, E., S. Schulte, and P.L. Richards. 2002. Impervious surfaces and water quality: a review of current literature and its implications for watershed planning. Journal of Planning Literature 16(4):499−514.

Cheng, Q., Z.W. Yan, and C.B. Fu. 2012. Climatic changes in the twenty−four solar terms during 1960−2008. Atmospheric Science 57(2−3):276−286.

Choi, G.Y., W.T Kwon, K.O. Boo, and Y.M. Cha. 2008. Recent spatial and temporal changes in means and extreme events of temperature and precipitation across the Republic of Korea. Journal of Korean Geographical Society 43(5):681−700 (최광용, 권원태, 부경온, 차유미. 2008. 최근 우리나라 기온 및 강수 평균과 극한 사상의 시·공간적 변화. 대한지리학회

지 43(5):681−700).

Choi, Y.E. 2004. Trends on temperature and precipitation extreme events in Korea. Journal of Korean Geographical Society 39(5):711−721 (최영은. 2004. 한국의 극한 기온 및 강수 사상의 변화 경향에 관한 연구. 대한지리학회지 39(5):711−721).

Choi, G.Y., W.T. Kwon, and D.A. Robinson. 2006. Seasonal onset and duration in South Korea. Journal of Korean Geographical Society 41(4):681−700 (최광용, 권원태, D. A. Robinson. 2006. 우리나라 사계절의 개시일과 지속기간. 대한지리학회지 41(4):435−456).

Coutts, A.M., J. Beringer, and N.J. Tapper. 2007. Impact of increasing urban density on local climate: spatial and temporal variations in the surface energy balance in Melbourne, Australia. American Meteorological Society 46(4):477−493.

Davis, J.C. 2002. Statistics and Data Analysis in Geology. John Wiley & Sons, Inc., New York, USA. p.268.

Deng, X., C.C. Zhao, and H. Yan. 2013. Systematic modeling of impacts of land use and land cover changes on regional climate: a review. Advances in Meteorology Volume 2013, Article ID 317678, http://dx.doi.org/10.1155/2013/ 317678.

Feddema, J.J., K.W. Oleson, G.B. Bonan, L.O. Mearns, L.E. Buja, G.A. Meehl, and W.M. Washington. 2005. The importance of land−cover change in simulating future climates. Science 310(5754):1674 −1678.

Hidore, J., J. Oliver, M. Snow, and R. Snow. 2010. Climatology−an Atmospheric Science. Prentice Hall, New York, USA. 293pp.

Hong, S.K. and C.S. Lee. 1997. Development and roles of landscape ecology as an emerging opportunity for ecology. The Korean Journal of Ecological Sciences 20(3):217−227 (홍선기, 이창석. 1997. 생태학의 새로운 분야로서 경관생태학의 발전과 역할. 한국생태학회지 20(3):217−227).

IPCC (Intergovernmental Panel on Climate Change). 2013. Climate Change 2013: The Physical Science Basis. In: Stocker, T.F., D. Qin, G.K. Plattner, M. Tignor, S.K. Allen, J. Boschung, A. Nauels, Y. Xia, V. Bex, and P.M. Midgley (ed.). Contribution of Working Group I to the Fifth Assessment Report of the Intergovernmental Panel on Climate Change. Cambridge University Press, New York, USA.

Jakubauskas, M.E., D.R. Legates, and J.H. Kastens. 2001. Harmonic analysis of time−series AVHRR NDVI data. Photogrammetric Engineering and Remote Sensing 67(4):461−470.

Jennings, D.B. and S.T. Jarnagin. 2002. Changes in anthropogenic impervious surfaces, precipitation and daily streamflow discharge: a historical perspective in a mid−atlantic subwatershed. Landscape Ecology 17(5):471−489.

Jeong, S.J., C.H. Ho, K.Y. Kim, and J.H. Jeong. 2009. Reduction of spring warming over East Asia associated with vegetation feedback. Geophysical Research Letters 36 L18705, doi:10.1029/2009GL039114.

Jin, M.J. and S.Y. Park. 2015. Temperature changes of climatic solar terms and their spatiotemporal characteristics in South Korea. Journal of the Korean Geographical Society 50(1):23−36 (진미정, 박선엽. 2015. 우리나라 기후 절기별 기온 변화의 시공간적 특성 분석. 대한지리학회지 50(1):23−36).

Jung, H.S., Y.E. Choi, J.H. Oh, and G.H. Lim. 2002. Recent trends in temperature and precipitation over South Korea. International Journal of Climatology 22(11):1327−1337.

Jung, S.K., J.H. Oh, and K.H. Park. 2005. A temporal structure analysis of forest landscape patterns using landscape indices in the Nakdong River Basin. Journal of the Korean Association of Geographic Information Studies 8(2):145−156 (정성관, 오정학, 박경훈. 2005. 경관지수를 활용한 낙동강 유역 산림경관의 시계열적 패턴 분석. 한국지리정보학회지 8(2):145−156).

Kang, Y.Q. and Y.S. Suh. 1986. Relationships between air temperature and sea surface temperature anomalies in Korea. Journal of Korean Meteorological Society 22(3):7−13.

Kim, H.S., H.B. Seok, and Y.K. Kim. 2014. A study on the change of the urban heat island structure in Busan metropolitan area, Korea. Journal of Environmental Science International 23(11):1807−1820 (김현수, 석현배, 김유근. 2014. 부산지역의 도시열섬 구조 변화에 관한 연구. 한국환경과학회지 23(11):1807−1820).

Kim, Y.J., H.S. Kim, Y.K. Kim, J.K. Kim, and Y.M. Kim. 2014. Evaluation of thermal environments during the heat waves of summer 2013 in Busan metropolitan area. Journal of Environmental Science International 23(11):1929−1941 (김영준,

김현수, 김유근, 김진국, 김영매. 2014. 2013년 부산지역 폭염사례일의 열쾌적성 평가. 한국환경과학회지 23(11):1929-1941).

Kondoh, A. and J. Nishiyama. 2000. Changes in hydrological cycle due to urbanization in the suburban of Tokyo metropolitan area, Japan. Advances in Space Research 26(7):1173-1176.

Kwon, Y.A. W.T. Kwon, K.O Boo, and Y.E. Choi. 2007. Future projections on subtropical climate regions over South Korea using SRES A1B data. Journal of Korean Geographical Society 42(3): 355-367 (권영아, 권원태, 부경온, 최경은. 2007. A1B 시나리오 자료를 이용한 우리나라 아열대 기후구 전망. 대한지리학회지 42(3): 355- 367).

Lee, W.J., M.K. Hwang, and Y.K. Kim. 2014. Health vulnerability assessment for PM10 in Busan. Journal of Environmental health Sciences 40(5):355-366 (이원정, 황미경, 김유근. 2014. 부산지역 미세먼지에 대한 건강 취약성 평가. 한국환경보건학회지 40(5): 355-366).

Lee, W.J. and M.K. Lee. 2016. Interannual variability of heat waves in South Korea and their connection with large-scale atmospheric circulation patterns. International Journal of Climatology 36(15):4815-4830.

NIMS (National Institute of Meteorological Sciences). 2010. Understanding climate change .Ⅴ. Korea Meteorological Administration (국립기상연구소. 2010. 기후변화 이해하기. V. 기상청).

Olsson L. and L. Eklundh. 1994. Fourier series for analysis of temporal sequences of satellite sensor imagery. International Journal of Remote Sensing 15(18):3735-3741.

Owen, T.W., T.N. Carlson, and R.R. Gillies. 1998. An assessment of satellite-sensed land cover parameters in quantitatively describing the climatic effect of urbanization. International Journal of Remote Sensing 19(9):1663-1681.

Park, B.I. 2011. The change of seasonal trend appeared in wintertime daily mean temperature of Seoul, Korea. Journal of Korean Geographical Society 46(2):152-167 (박병익. 2011. 서울의 겨울철 일평균 기온에 나타난 계절 추이의 변화. 대한지리학회지 46(2):152-167).

Park, H.M. and T.K. Baek. 2009. Progress and land-use characteristics of urban sprawl in Busan metropolitan city using remote sensing and GIS. Journal of Korean Association of Geographic Information Studies 12(2):23-33 (박호명, 백태경. 2009. 원격탐사와 GIS를 이용한 부산광역시 도시화지역의 확산과정과 토지이용 특성에 관한 연구. 한국지리정보학회지 12(2):23- 33).

Park, S.Y. 2003. Harmonic analysis of NDVI response patterns to temporal changes in soil moisture content. The Korean Association of Professional Geographers 37(1):67-79.

Park, S.Y. 2009. Synchronicity between satellite-measured leaf phenology and rainfall regime in Hawaiian tropical forests. Photogrammetric Engineering and Remote Sensing 75(10):1231-1237.

Park, S.Y. 2010. A dynamic relationship between the leaf phenology and rainfall regimes of Hawaiian tropical ecosystems:

a remote sensing approach. Singapore Journal of Tropical Geography 31(3): 371−383.

Park, S.Y. and H.M. Tak. 2013. Land use changes and climate patterns in Southeast Korea. Journal of Korean Association of Geographic Information Studies 16(2):47−64 (박선엽, 탁한명. 2013. 우리나라 동남부 지역의 토지 이용과 기후 패턴 변화 분석. 한국지리정보학회지 16(2):47−64).

Pielke, R.A., G. Marland, R.A. Betts, T.N. Chase, J.L. Eastman, J.O. Niles, D.S. Niyogi, and S.W. Running. 2002. The influence of land−use change and landscape dynamics on the climate system: relevance to climate−change policy beyond the radiative effect of greenhouse gases. Philosophical Transactions of the Royal Society of London A 360(1797):1705−1719.

Qian, C., Z. Yan, and C. Fu. 2012. Climatic changes in the twenty−four solar terms during 1960−2009. Atmospheric Science 57(2−3):276−286.

Seto, K.C. and M. Fragkias. 2005. Quantifying spatiotemporal patterns of urban land−use change in four cities of China with time series landscape metrics. Landscape Ecology 20(7):871−888.

Stine, A.R., P. Huybers, and I.Y. Fung. 2009. Changes in the phase of the annual cycle of surface temperature. Nature 457(7228):435−441.

Stone Jr., B. 2009. Land use as climate change mitigation. Environmental Science and Technology 43(24):9052−9056.

Stone, B. and M.O. Rodgers. 2001. Urban form and thermal efficiency−how the design of cities influence the urban heat island effect. Journal of the American Planning Association 67(2):186−198.

Thomson, D.J. 1995. The seasons, global temperature, and precession. Science 268(5207):59−68.

Wilks, D.S. 2011. Statistical Methods in the Atmospheric Sciences. Elsevier, Oxford, UK. pp.428−438. **KAGIS**